XIII International Workshop on Hadron Physics IOP Publishing
Journal of Physics: Conference Series **706** (2016) 052026 doi:10.1088/1742-6596/706/5/052026

Cold quark matter phase diagram under strong magnetic fields within a generalized SU(2) NJL model

PG Allen[a], VP Pagura[b,c,d] and NN Scoccola[a,b,e]

[a] Department of Theoretical Physics, Comisión Nacional de Energía Atómica, Av.Libertador 8250, 1429 Buenos Aires, Argentina
[b]CONICET, Rivadavia 1917, 1033 Buenos Aires, Argentina
[c]IFLP, CONICET-Dpto. de Física, Univ.Nac. de La Plata, C.C.67, (1900) La Plata, Argentina
[d] Dpto. de Física Teórica-IFIC, Univ. de Valencia-CSIC, E-46100 Burjassot, Valencia, Spain
[e] Universidad Favaloro, Solís 453, 1078 Buenos Aires, Argentina

E-mail: allen@tandar.cnea.gov.ar

Abstract. We study the effect of intense magnetic fields on the phase diagram of cold, strongly interacting matter within an extended version of the Nambu-Jona-Lasinio model that includes flavor mixing effects and vector interactions. Different values of the relevant model parameters in acceptable ranges are considered. Charge neutrality and beta equilibrium effects, which are specially relevant to the study of compact stars, are also taken into account. In this case the behavior of leptons is discussed.

1. Introduction

The influence of intense magnetic fields on the properties of strongly interacting matter has become an issue of increasing interest in recent years [1]. This is mostly motivated by the realization that in some relevant physical situations, like high energy non-central heavy ion collisions [2] and compact stellar objects called magnetars [3], very strong magnetic fields may be produced. Since in these systems extreme temperatures and/or densities may be found, it is interesting to investigate which modifications are induced by the presence of strong magnetic fields on the whole QCD phase diagram. Unfortunately, even in the absence of those fields, the present knowledge of such phase diagram is only schematic due to the well-known difficulty given by the so-called sign problem which affects lattice calculations at finite chemical potential [4]. Of course, the presence of strong magnetic fields makes the situation even more complex. Thus, most of our present knowledge of their effect comes from investigations performed in the framework of effective models [5]. In this contribution we present some results of a study of the phase diagram of cold quark matter subject to intense magnetic fields in the framework of a generalized Nambu-Jona-Lasinio (NJL) model. The NJL-type models are effective relativistic quark models for non-perturbative QCD, where gluon degrees of freedom are integrated out and interactions are modelled through point-like interactions. In its simplest version [6] it only includes scalar and pseudo-scalar interactions that describe chiral symmetry breaking effectively. As is well known, however, a more detailed description of the low-energy quark dynamics requires that other channels like flavor-mixing and vector-meson interactions are taken into

account [7]. In fact, some aspects of the effect of those interactions on the magnetized quark matter have already been investigated [8, 9]. The purpose of this work is to extend those analyzes by performing a detailed study of the resulting cold matter phase diagrams, including their dependence on the parameters that regulate the strength of these interactions. Moreover, the behavior of cold magnetized quark matter under $\beta-$equilibrium with leptons will be considered, condition relevant for the physics of compact stars.

This contribution is organized as follows. In Sec. 2 we provide some details of the model and its parametrizations as well as the way to deal with an external constant magnetic field. In Sec. 3 we discuss our results for symmetric quark matter. The situation for neutral matter is analyzed in Sec. 4. Our conclusions are given in Sec. 5.

2. Formalism

We consider the most general SU(2) Lagrangian density which includes a scalar-pseudoscalar interaction, vector-axial vector and the t´Hooft determinant interaction [7]. In the presence of an external magnetic field and chemical potential it reads:

$$\mathcal{L} = \bar{\psi}\left(i \not{D} - m_c + \hat{\mu}\,\gamma^0\right)\psi + \mathcal{L}_{int} \tag{1}$$

where

$$\begin{aligned}\mathcal{L}_{int} &= G_1 \sum_{a=0}^{3}\left[\left(\bar{\psi}\tau_a\psi\right)^2 + \left(\bar{\psi}i\gamma_5\tau_a\psi\right)^2\right] + G_2\sum_{a=0}^{3}\left[\left(\bar{\psi}\gamma_\mu\tau_a\psi\right)^2 + \left(\bar{\psi}\gamma_\mu\gamma_5\tau_a\psi\right)^2\right] \\ &+G_3\left[\left(\bar{\psi}\gamma_\mu\psi\right)^2 + \left(\bar{\psi}\gamma_\mu\gamma_5\psi\right)^2\right] + G_4\left[\left(\bar{\psi}\gamma_\mu\psi\right)^2 - \left(\bar{\psi}\gamma_\mu\gamma_5\psi\right)^2\right] + 2G_D\left(d_+ + d_-\right)\end{aligned} \tag{2}$$

Here, G_i with $i = 1, 4$ and G_D are coupling constants, $\psi = (u, d)^T$ represents a two-flavor quark field with two flavors, $d_\pm = det\left[\bar{\psi}\left(1 \pm \gamma_5\right)\psi\right]$, $\hat{\mu} = \mathrm{diag}\left(\mu_u, \mu_d\right)$ the quark chemical potentials, m_c is the (current) mass matrix that we take to be the same for both flavors , $\tau_0 = I_{2\times2}$, and τ_a, $0 < a \leq 3$ denote the Pauli matrices. The coupling of the quarks to the electromagnetic field $\mathcal{A}_\mu$ is implemented through the covariant derivative $D_\mu = \partial_\mu - i\hat{q}\mathcal{A}_\mu$ where $\hat{q}$ represents the quark electric charge matrix $\hat{q} = \mathrm{diag}\left(q_u, q_d\right)$ where $q_u/2 = -q_d = e/3$. We consider a static and constant magnetic field in the 3-direction, $\mathcal{A}_\mu = \delta_{\mu 2}x_1 B$. In the mean-field approximation the grand-canonical thermodynamical potential reads

$$\Omega^{\mathrm{MFA}} = -\sum_{f=u,d}\theta_f + \Omega_{pot} \tag{3}$$

where θ_f gives the contribution from the gas of quasi-particles of each flavor $f = u, d$ and can be written as the sum of 3 contributions [10]

$$\begin{aligned}\theta_f^{\mathrm{vac}} &= \frac{N_c}{8\pi^2}\left\{\Lambda\left(2\Lambda^2 + M_f^2\right)\sqrt{\Lambda^2 + M_f^2} - M_f^4 \ln\left[\frac{(\Lambda + \sqrt{\Lambda^2 + M_f^2})}{M_f}\right]\right\}, \\ \theta_f^{\mathrm{mag}} &= \frac{N_c}{2\pi^2}\left(|q_f|B\right)^2\left[\zeta^{(1,0)}(-1, x_f) - \frac{1}{2}(x_f^2 - x_f)\ln x_f + \frac{x_f^2}{4}\right], \\ \theta_f^{\mathrm{med}} &= \frac{N_c}{4\pi^2}\,|q_f|B\sum_{\nu=0}^{\nu_f^{max}}\alpha_\nu\left[\tilde{\mu}_f\sqrt{\tilde{\mu}_f^2 - s_f(\nu,B)^2}\right. \\ &\qquad\left. - s_f(\nu,B)^2\ln\left(\frac{\tilde{\mu}_f + \sqrt{\tilde{\mu}_f^2 - s_f(\nu,B)^2}}{s_f(\nu,B)}\right)\right],\end{aligned} \tag{4}$$

where $M_f = m_c + \sigma_f$ and $\tilde{\mu}_f = \mu_f - \omega_f$, with σ_f and ω_f being the mean field values of the scalar and vector meson fields, respectively. Λ represents a non covariant ultraviolet cutoff and $\zeta^{(1,0)}(-1, x_f) = d\zeta(z, x_f)/dz|_{z=-1}$ where $\zeta(z, x_f)$ is the Riemann-Hurwitz zeta function. In addition, $s_f(\nu, B) = \sqrt{M_f^2 + 2|q_f|B\nu}$ while $x_f = M_f^2/(2|q_f|B)$. In θ_f^{med}, the sum is over the Landau levels (LLs), represented by ν, while $\alpha_\nu = 2 - \delta_{\nu 0}$ is a degeneracy factor and ν_f^{max} is the largest integer that satisfies $\nu_f^{max} \leq (\tilde{\mu}_f^2 - M_f^2)/(2|q_f|B)$.

The Ω_{pot} contribution reads

$$\Omega_{pot} = \frac{(1-c_s)(\sigma_u^2 + \sigma_d^2) - 2c_s\,\sigma_u\,\sigma_d}{8g_s(1-2c_s)} - \frac{(1-2c_v)(\omega_u^2 + \omega_d^2) + c_v\,\omega_u\,\omega_d}{8g_v(1-2c_v)} \tag{5}$$

where we have introduced a convenient parametrization of the coupling constants in terms of the quantities g_s, c_s, g_v and c_v given by

$$g_s = G_1 + G_D, \quad g_v = G_2 + G_3 + G_4, \quad c_s = \frac{G_D}{G_1 + G_D}, \quad c_v = \frac{G_3 + G_4}{2(G_2 + G_3 + G_4)}. \tag{6}$$

The relevant gap equations are given by

$$\frac{\partial \Omega^{\rm MFA}(\sigma_u, \sigma_d, \omega_u, \omega_d)}{\partial(\sigma_u, \sigma_d, \omega_u, \omega_d)} = 0\ . \tag{7}$$

In our calculations we will consider first the simpler case of symmetric matter where both quarks carry the same chemical potential μ. Afterwards, we will analyze the case of neutral matter in which leptons are also present and β-equilibrium and charge neutrality are imposed. In this case the chemical potential for each quark, μ_f, is a function of μ and the lepton chemical potentials which have to be selfconsistently determined.

We will consider two SU(2) NJL model parametrizations: set 1, with $m_c = 5.595$ MeV, $g_s\Lambda^2 = 2.212$, $\Lambda = 620.9$ MeV, corresponds to that leading to $M_0 = 340$ MeV; and set 2, with $m_c = 5.833$ MeV, $g_s\Lambda^2 = 2.44$, $\Lambda = 587.9$ MeV, to that leading to $M_0 = 400$ MeV. Here M_0 is the vacuum quark effective mass in the absence of external magnetic field.

The presence of the t'Hooft determinant interaction reflects the $U_A(1)-$anomaly of QCD. Its strength, and consequently the amount of flavor mixing induced by this term, is controlled by the parameter c_s. An estimate for its value can be obtained from the $\eta - \eta'$ mass splitting within the 3−flavor NJL model [11]. This leads to $c_s \simeq 0.2$ [12]. In any case, to obtain a full understanding of the effects of flavor mixing we will vary the value of c_s in a range going from 0, which corresponds to a situation in which the two flavors are completely decoupled, to 0.5, being this the case of maximum flavor mixing described in Ref. [13]. Regarding the vector coupling constant g_v, we recall that one can obtain naturally the vector axial-vector interaction if one starts from a QCD-inspired color current-current interaction and then performs a Fierz transform into color-singlet channels, and that in this case the relation between coupling strengths is $g_v = g_s/2$ [7]. Yet, the value of g_v cannot be accurately determined from experiments nor from lattice QCD simulations and this is why it has been taken as a free parameter in most works. In the present work we take $0 < g_v/g_s < 0.5$.

3. Results for symmetric matter

In this section we present the results for the case of symmetric matter, obtained by solving the set of coupled "gap equations", Eqs. (7), for different values of magnetic field and chemical potential. We will consider in Sec. 3.1 the effect of flavor mixing on quark behavior in the absence of vector interactions and turn to the study of the role of those interactions in Sec. 3.2.

3.1. Effect of the flavor mixing interactions

Neglecting vector interactions implies taking $G_2 = G_3 = G_4 = 0$ in Eq. (2), while $G_1 \neq 0$ and $G_D \neq 0$. Therefore, Eqs. (7) will become a set of two coupled equations that must be solved for the independent variables M_u and M_d. The parameter c_s acts as a coupling between both flavors and we study how the phase transitions are modified as we vary this parameter.

The case $c_s = 0.5$ corresponds to ordinary NJL described in detail in Ref [13], where both flavors have identical behavior. If $c_s < 0.5$, then both masses will be independent variables, and transitions for each flavor might occur simultaneously or not in different regions of the phase diagrams. It is common to all these cases that chiral symmetry is completely broken for chemical potentials well below M_0 and that restoration occurs for high enough chemical potentials, usually accompanied by a large drop in the dressed mass. The inclusion of a constant magnetic field modifies the quark dispersion relation, introducing LL's into its spectrum. As a consequence, chiral symmetry restoration occurs in several steps, each of which is a transition where quark population appears on previously unoccupied LL's, giving rise to a potentially complex phase diagram, whose precise form depends on the parameter set and magnetic field.

We will start by analyzing the phase transitions for the case with no flavor mixing, i.e. $c_s = 0$, previously studied in Ref. [8]. The phase diagrams for both parameter sets can be seen in the upper two panels of Fig. 1. In a sense, each flavor will have its own independent phase diagram because the gap equations are decoupled. Here, each line corresponds to a transition where LL population of a single quark flavor occurs (red lines for down quarks, blue lines for up quarks). Both flavors will coincide for $eB = 0$ where $SU(2)$ symmetry is recovered and behave differently as eB increases, due to their different electric charges. Both diagrams are related through a scale change $eB \to 2eB$.

When c_s becomes finite (second row onwards in Fig. 1), flavors become coupled and a complex pattern is created, where transitions move closer together in some regions and even merge together in others, that is, the LL population changes simultaneously for both flavors (these are represented by black lines). We can see that already for $c_s = 0.03$, the transitions occur together for low magnetic fields, and then separate for $B = 0.02$ GeV^2 in set 1 and 0.1 GeV^2 in set 2.

For a better understanding of the meaning of the transition lines, we present in Fig. 2 the dressed masses for both flavors for set 2, $c_s = 0.03$ and $eB = 0.11$ GeV^2. When the first discontinuity is encountered at $\mu = 370$ MeV, M_u jumps to half its value and its lowest LL (LLL) becomes populated. On the other hand, the down flavor remains in vacuum. Actually, its mass presents a small discontinuity caused by the weak coupling to the up quark which is not to be confused with a down transition, that effectively occurs at $\mu = 374$ MeV. When both flavors are in the vacuum phase, $M_u > M_d$, while in the populated phase it happens the other way around, which is consistent with the phenomena of catalysis/anticatalysis discussed in Ref. [13].

For $c_s = 0.2$, the transitions for both flavors occur together, so the qualitative behavior is very similar to the full flavor mixing case $c_s = 0.5$. In fact, the model tends to full mixing quite quickly and only for $c_s \lesssim 0.1$ are relevant mixture effects (or more precisely, the absence of it) actually seen. On the other hand, cross over transitions do not have this property and tend much more slowly to the $c_s = 0.5$ behavior.

3.2. Effect of the vector interactions

In this section we analyze the effect of vector interaction terms. Since for $c_s \gtrsim 0.1$ the phase diagrams do not present qualitative variations we fix $c_s = 0.2$, which is also in the range of realistic values suggested in Ref. [12]. Although our results correspond to $c_v = 0$, we have shown that only small quantitative differences occur when varying this parameter from 0 to 1.

In Fig. 3 we present a series of phase diagrams obtained for different values of the ratio g_v/g_s. For set 1 we observe that as g_v/g_s increases the two lower and main transitions separate and several new transitions appear in the low eB region of the diagram. For set 2 at some small

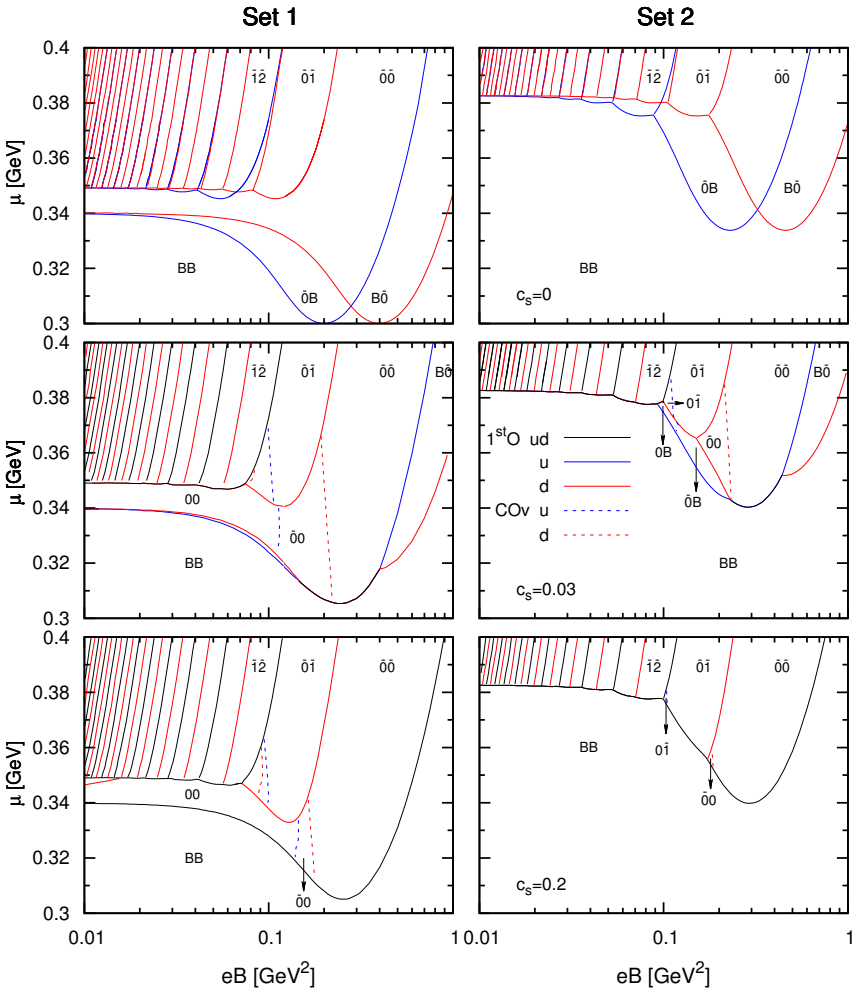

Figure 1. (Color online) Phase diagrams in the $eB-\mu$ plane for the case of symmetric matter with different values of flavor-mixing parameter c_s and no vector interactions. To simplify the figure we have introduced a compact notation to indicate the phases. The pair of integers mn corresponds to the C_{mn} phase and the pair $\bar{m}\bar{n}$ to the A_{mn} phase. The case in which one quark is in a C-type phase and the other in the A-type phase is indicated by putting a bar on top of the integer associated with the A-type phase.

$g_v/g_s \simeq 0.1$ the lower transition first splits into two, leaving a 00 phase in between which was not present before. For larger values of g_v/g_s the behavior is similar to that of set 1. In fact, increasing the vector interaction coupling has the same effect as going to a parameter set that reproduces a lower value of current mass M_0, described in Ref. [13]. Notice that the phase diagram for set 2 and $g_v/g_s = 0.3$ is in this sense very similar to set 1 and $g_v/g_s = 0$. The well-shaped behavior of the lowest transition is a manifestation of inverse magnetic catalysis (IMC), effect that is reduced with increasing g_v.

4. Results for neutral matter under $\beta-$equilibrium

We now turn our attention to stellar matter, fixing as in the previous section $c_s = 0.2$. If charge neutrality is imposed on our system, there will be a fixed relation between the densities of the up and down quarks, which will be necessarily different unless they are both zero. So, even though

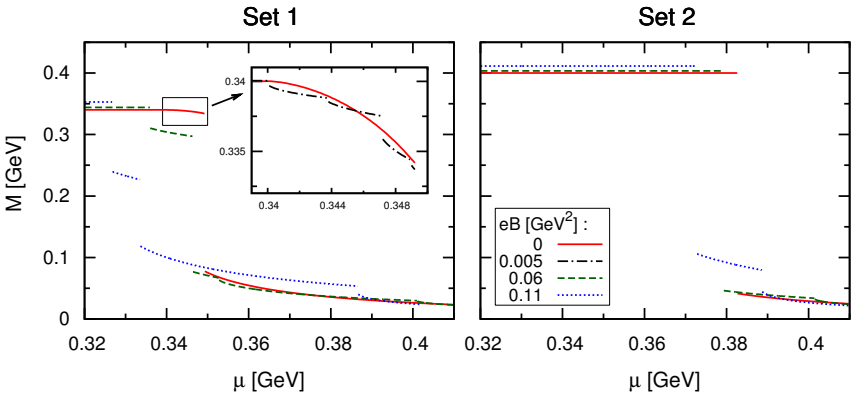

Figure 2. (Color online) Dressed mass as function of chemical potential for different values of magnetic field in the case of symmetric matter with maximum flavor mixing and no vector interactions, for both parameter sets.

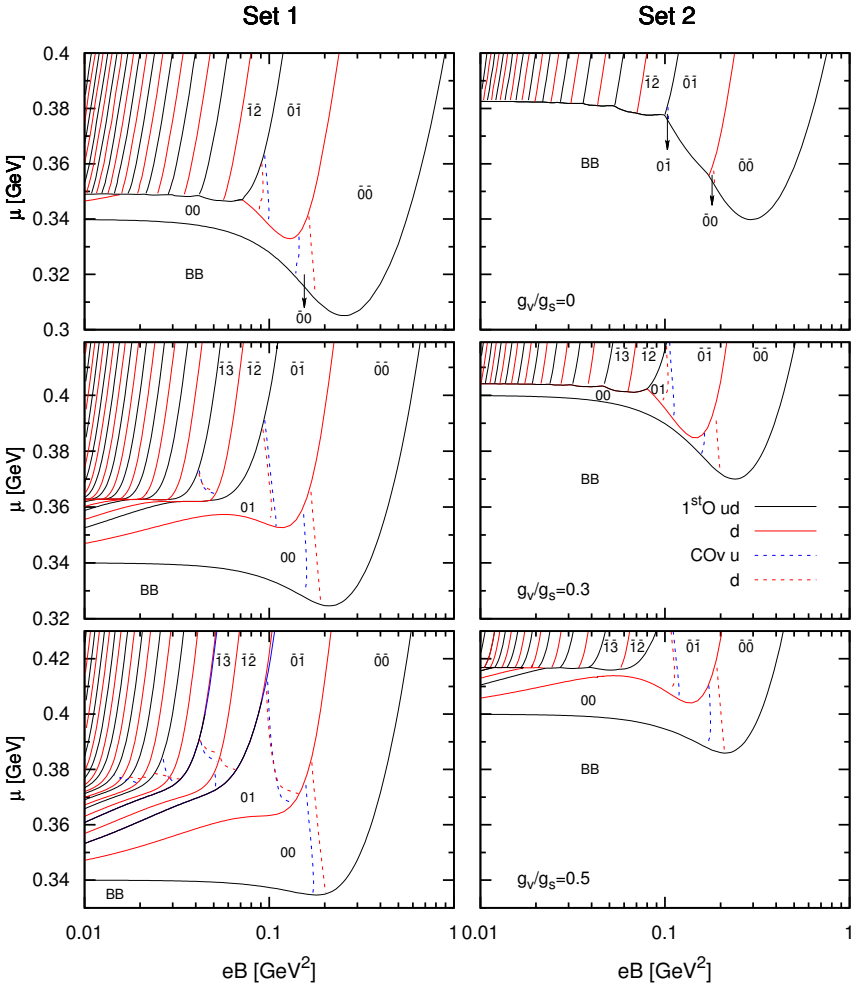

Figure 3. (Color online) Phase diagrams in the $eB-\mu$ plane for symmetric matter with $c_s = 0.2$ and different values of g_v/g_s. Phases are denoted as explained in Fig. 1.

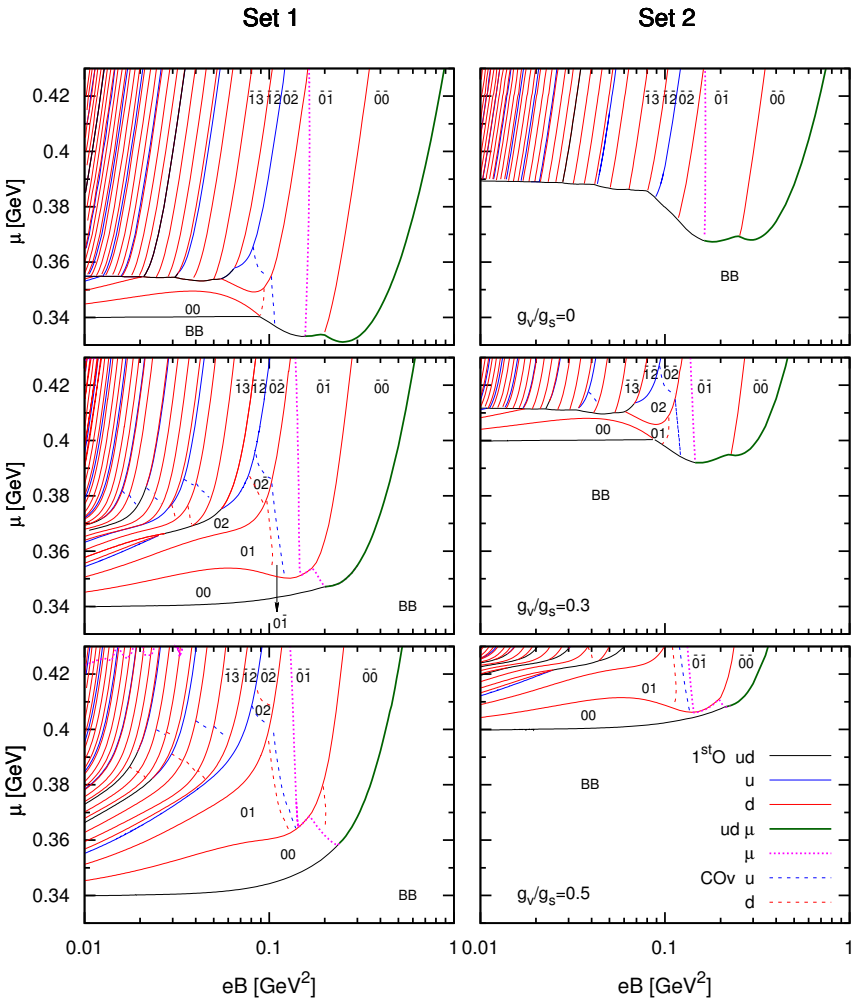

Figure 4. (Color online) Phase diagrams in the $eB - \mu$ plane for neutral matter under β-equilibrium with $c_s = 0.2$ and different values of g_v/g_s. Phases are denoted as explained in Fig. 1. The pink dotted line represents muon transition from vacuum to LLL.

$c_s = 0.2$ was close enough to the full mixing case according to what was established in previous sections, charge neutrality will cause the flavors to behave differently among themselves.

The phase diagrams in the $eB - \mu$ plane for both parameter sets and for increasing values of g_v are plotted in Fig. 4. The chemical potential μ on the horizontal axis is now the quark number chemical potential, which is related to flavor chemical potentials through $\mu_f = \mu - q_f \mu_e$. The introduction of charge neutrality has a few effects similar to those of vector interaction, in the sense that diagrams become similar to the ones corresponding to lower M_0 sets: main transitions separate for low eB and several transitions appear in the region between them. The magnetic anticatalysis effect is reduced also: The depth of the anticatalysis well, as defined in the previous section, is reduced from 35 MeV to 9 MeV in set 1 and from 43 MeV to 22 MeV in set 2. As expected, the introduction of vector interactions will further enhance these effects, so that anticatalysis has completely disappeared for $g_v = 0.5$.

The "Van Alphen - de Haas" (VA-dH) transitions acquire relatively independent behaviors when charge neutrality is introduced. In particular, for intermediate $eB\,(\simeq 0.1\ \mathrm{GeV}^2)$ the transition between $k_u = 0$ and $k_u = 1$ is well separated from the down transition. For symmetric

matter, the VA-dH transitions occurred to a very good level of approximation for a critical chemical potential $\mu_c = \sqrt{2kq_fB}$ (being this condition exact for the chiral case), so the relation between the charges produced one up transition every two down transitions. Although this relation is still satisfied for each flavor chemical potential, these are now different between themselves and related through $\mu_u - \mu_d + \mu_e = 0$. As a result of this, in Fig. 4 we roughly have one up transition every four down transitions. With respect to the leptons, it is seen that the electron LLL becomes populated simultaneously with quarks, while the muon transition presents a more complicated dependence with the magnetic field. Namely, the muon LLL requires a very high chemical potential to become populated at low eB, however, the critical μ drops suddenly at intermediate magnetic fields and joins the main quark transition together with electrons.

5. Final Comments

We have investigated how the phase diagram of cold strongly interacting matter is modified in the presence of intense magnetic fields in the context of NJL-type models which include flavor mixing and vector interaction. The whole range of possible flavor mixing values was swept through, going from the situation in which the two flavors are completely decoupled, to the one in which they are fully mixed. For low mixing values, a complex phase diagram is generated, but already for $c_s \simeq 0.1$, phase diagrams display a behavior that is qualitatively very similar to the full mixing case. Since SU(3) estimates suggest a value of $c_s \simeq 0.2$, it can be concluded that the realistic flavor mixing range is similar in behavior to the full mixing case. In what followed, vector interactions and the conditions of β-equilibrium and charge neutrality were introduced. The most notable effect observed is that they attenuate the IMC phenomenon, to the point that it completely disappears when both effects are jointly taken into account. It was also found that introducing vector interaction causes the two main transitions to separate and additional phases to appear between these two, effects that are similar to those occurring when changing to a parameter set that fits to a smaller dressed mass.

Acknowledgments

This work was partially supported by CONICET (Argentina) under grant PIP 00682, by ANPCyT (Argentina) under grant PICT-2011-0113 and by the Mineco (Spain) under contract FPA2013-47443-C2-1-P and CPAN(CSD- 00042) and by Generalitat Valenciana (Spain) under contract PrometeoII/2014/066.

References

[1] Kharzeev D E, Landsteiner K, Schmitt A and Yee H-U 2013 *Lect. Notes Phys.* **871**, 1.
[2] Kharzeev D E , McLerran L D and Warringa H J 2008 *Nucl. Phys.* **A803**, 227.
[3] Duncan R C and Thompson C 1992 Astrophys J. 392, L9.
[4] Karsch F, Laermann E, 2004 *Quark Gluon Plasma 3*, ed.by R.C.Hwa et al. (World Scientific Singapore), p.1.
[5] Fraga E S 2013 *Lect. Notes Phys.* **871**, 121; Gatto R and Ruggieri M, 2013 *Lect. Notes Phys.* **871**, 87; Ferrer E J and de la Incera V 2013 *Lect. Notes Phys.* **871**, 399.
[6] Nambu Y and Jona-Lasinio G 1961 *Phys. Rev.* **122**, 345; 1961 **124**, 246.
[7] Vogl U and Weise W 1991 *Prog. Part. Nucl. Phys.* **27**, 195; Klevansky S 1992 *Rev. Mod. Phys.* **64**, 649; Hatsuda T and Kunihiro T 1994 *Phys. Rep.* **247** 221.
[8] Boomsma J K and Boer D 2010 *Phys. Rev.* D **81**, 074005.
[9] Denke R Z and Pinto M B 2013 *Phys. Rev.* D **88**, 056008 ;
Menezes D P, Pinto M B, Castro L B, Costa P and Providência C 2014 *Phys. Rev.* C **89**, 055207.
[10] Menezes D P, Pinto M B, Avancini S S, Pérez Martínez A and Providência C 2009 *Phys. Rev.* **C 79** 035807; Menezes D P, Pinto M B, Avancini S S and Providência C 2009 *Phys. Rev.* **C 80** 065805; Avancini S S, Menezes D P and Providência C 2011 *Phys. Rev.* **C 83**, 065805.
[11] Kunihiro T 1989 *Phys. Lett.* B **219**, 363 1990 [*Erratum-ibid.* B **245**, 687].
[12] Frank M, Buballa M and Oertel M 2003 *Phys. Lett.* B **562**, 221.
[13] Allen P G and Scoccola N N Phys. Rev. D **88**, 094005 (2013).